Analytica Chimica Acta 1261 (2023) 341209

Contents lists available at ScienceDirect

Analytica Chimica Acta

journal homepage: www.elsevier.com/locate/aca

A MEMS-enabled portable gas chromatography injection system for trace analysis

Nipun Thamatam [a], Jeonghyeon Ahn [a,b], Mustahsin Chowdhury [a], Arjun Sharma [c], Poonam Gupta [c], Linsey C. Marr [b], Leyla Nazhandali [c], Masoud Agah [a,*]

[a] VT MEMS Lab, The Bradley Department of Electrical and Computer Engineering, Virginia Polytechnic Institute and State University, Blacksburg, VA, 24061, United States

[b] Department of Civil and Environmental Engineering, Virginia Polytechnic Institute and State University, Blacksburg, VA, 24061, United States

[c] CESCA, The Bradley Department of Electrical and Computer Engineering, Virginia Polytechnic Institute and State University, Blacksburg, VA, 24061, United States

HIGHLIGHTS

- Novel removable gas-tight fluidic connections for microfluidic chips with sideports
- Swappable micropreconcentrator cartridge to mimic sorbent tube for trace analysis.
- Highly versatile thermal desorption and injection unit for gas chromatography.
- Split injection control for dilution and sharp injection (plug widths ≈ 240 ms).
- Detection of analytes with concentrations of <100 ppt within 20 min of sampling.

GRAPHICAL ABSTRACT

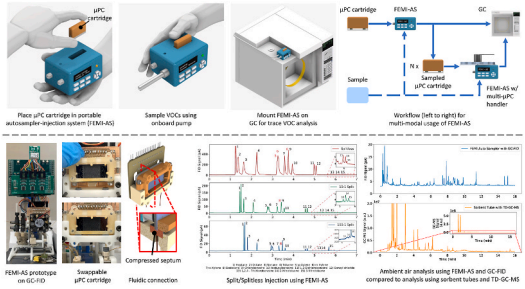

ARTICLE INFO

Keywords:
Gas chromatography
Trace analysis
Volatile organic compounds
Portable thermal desorption unit
Micropreconcentrator
Fluidic connections

ABSTRACT

Growing concerns about environmental conditions, public health, and disease diagnostics have led to the rapid development of portable sampling techniques to characterize trace-level volatile organic compounds (VOCs) from various sources. A MEMS-based micropreconcentrator (μPC) is one such approach that drastically reduces the size, weight, and power constraints offering greater sampling flexibility in many applications. However, the adoption of μPCs on a commercial scale is hindered by a lack of thermal desorption units (TDUs) that easily integrate μPCs with gas chromatography (GC) systems equipped with a flame ionization detector (FID) or a mass spectrometer (MS).

Here, we report a highly versatile μPC-based, single-stage autosampler-injection unit for traditional, portable, and micro-GCs. The system uses μPCs packaged in 3D-printed swappable cartridges and is based on a highly modular interfacing architecture that allows easy-to-remove, gas-tight fluidic, and detachable electrical connections (FEMI). This study describes the FEMI architecture and demonstrates the FEMI-Autosampler (FEMI-AS) prototype (9.5 cm × 10 cm x 20 cm, ≈500 gms). The system was integrated with GC-FID, and the performance was investigated using synthetic gas samples and ambient air. The results were contrasted with the sorbent tube sampling technique using TD-GC-MS. FEMI-AS could generate sharp injection plugs (≈240 ms) and detect analytes with concentrations <15 ppb within 20 s and <100 ppt within 20 min of sampling time. With more than

* Corresponding author.
E-mail address: agah@vt.edu (M. Agah).

https://doi.org/10.1016/j.aca.2023.341209
Received 21 December 2022; Received in revised form 18 March 2023; Accepted 10 April 2023
Available online 19 April 2023

30 detected trace-level compounds from ambient air, the demonstrated FEMI-AS, and the FEMI architecture significantly accelerate the adoption of μPCs on a broader scale.

1. Introduction

Volatile organic compounds (VOCs) are carbon-based compounds with high vapor pressures at room temperature [1]. They are ubiquitous and provide rich information about ecological, environmental, physiological, and manufacturing processes [2–6]. For instance, biogenic VOCs are highly diverse and participate in biosynthesis, plant defense, and atmospheric chemistry that affects air quality and climate [7,8]. These include isoprenoids, alkanes, alkenes, carbonyls, alcohols, esters, ethers, and acids [9,10]. Similarly, anthropogenic VOCs, such as aromatics and oxygenates, are essential ingredients or byproducts of various consumer products such as paints, pharmaceuticals, and fossil fuels [11–13]. Some anthropogenic VOCs, with atmospheric concentrations ranging between a few ppt to several ppb, readily oxidize to form aerosol precursor compounds that significantly impact air quality and play a significant role in ozone formation, a key contributor to photochemical smog. Furthermore, exposure to VOCs such as BTEX (Benzene, Toluene, Ethylbenzene, and Xylenes) and hexane may have short-term and long-term adverse health effects [14–16].

On the other hand, studies have shown that VOCs emanating from humans, animals, and plants reflect the internal physiological status for use in non-invasive disease diagnostics [17–19]. VOC analysis has produced promising diagnostic results for asthma, ovarian cancer, and chronic obtrusive pulmonary disease (COPD), among other conditions [20–25]. Similarly, disease diagnosis in cattle and other domesticated animals using breath analysis has been an emerging approach for animal health management [26]. Also, a significant effort has been made to characterize biogenic VOCs for plant phenotyping and identifying plant disease markers [27]. In addition, VOCs emitted by food are measured for uses in food production, quality control, flavor, and food storage [28]. Therefore, collecting and analyzing trace-level VOCs in gaseous matrices emanating from various sources is immensely important in numerous disciplines for many applications.

VOCs are typically analyzed using well-established gas chromatography (GC) systems equipped with mass spectrometry (MS) or flame ionization detectors (FID). Analytical tools such as portable GCs, micro-GCs, and electronic noses have also been developed to allow in-situ analysis [29–33]. However, detecting trace-level VOCs (<0.5 ppm) has been challenging in all analytical systems. Detection has been constrained by the detector's sensitivity and the system's limit of detection (LOD). While substantial developmental efforts have been made to improve the detector's sensitivity, sample collection and preconcentration for enhancing the system's LOD remains the first critical step in trace-level VOC analysis workflow.

Typically, whole gas samples with trace analytes are collected using sample containers such as Tedlar bags and vacuum canisters. The containers are then transported to a laboratory for off-site preconcentration and sample analysis. This method often involves careful storage and transport, increasing the risk of sample loss, contamination, and degradation [34,35]. To mitigate these issues and to enable direct in-situ sampling, commercially available sorbent tubes packed with adsorbents have been developed since the 1970s [36–41]. However, their relatively large size and manufacturing cost lower the sampling flexibility in some applications. Additionally, sorbent tubes require expensive benchtop thermal desorption units (TDU) and cold traps for sample desorption and injection. These desorption systems are power intensive, need heated transfer lines, use large carrier gas volumes, and take a long time (5–15 min) for complete desorption. High resource requirements and long processing times may increase the cost per sample significantly and make them incompatible with portable GCs and micro-GCs applications.

Developments in miniaturized active and passive sampling techniques compatible with all GC platforms have addressed some of these issues. Sampling techniques, such as needle trap microextraction, in-tube extraction, solid-phase microextraction (SPME) fibers, and needle trap devices, have a more straightforward operation, use fewer resources, and have shorter processing times [42]. However, unlike TDUs, they are operated manually and are unsuitable for unattended use. Efforts to develop a single-stage field-deployable TDU have been appreciable [43,44]. Yet, they are based on redesigned sorbent tubes and are awkward for biosensing applications such as diagnostics based on skin or plant emissions.

Micropreconcentrators (μPC) fabricated using micro-electromechanical systems (MEMS) technology drastically reduce the size, manufacturing cost, processing time, and power consumption. Their small form factor provides greater scope for implementation in many environmental and biosensing applications. Tremendous flexibility in device design and adsorbents allows for novel system implementations such as active, passive, multi-bed, and selective preconcentration [45–52]. Recent studies have shown that μPCs produce promising results for trace-level analysis of air and breath with analyte concentrations as low as 1 ppb [53]. However, the adoption of μPC on a broader scale is stifled by a lack of reliable easy-to-remove fluidic connections. Currently, the fluidic connections for μPCs are established using Nanoport assemblies for devices with top ports or by gluing capillary tubes using thermally resistive adhesives for side ports. Standard compression fittings connect μPC with attached capillary tubes to the rest of the analytical system. While the connections are removable in some cases, they introduce sizeable dead volume, are susceptible to breakage, and lack the usability necessary for μPC use as a removable preconcentrator across all scales of GC platforms.

To the authors' knowledge, no portable thermal desorption system has been developed to enable a MEMS-based μPC to act as a modular injection unit for various gas chromatography systems. Therefore, we envision a highly versatile μPC based single-stage autosampler for collecting and processing trace-level VOCs. The system is expected to work with a swappable μPC cartridge built on a novel architecture that allows easy-to-remove gas-tight fluidic and detachable electrical connections. The architecture is called a Fluidic and Electrical Modular Interfacing (FEMI) architecture, and the autosampler is dubbed a Fluidic and Electrical Modular Interfacing-Autosampler (FEMI-AS). Fig. 1 shows the general workflow of the FEMI-AS concept in various operational modes with the ability to automatically process multiple μPCs for unattended use.

This work describes the FEMI architecture and presents the first-generation FEMI-AS that is 9.5 cm × 10 cm x 20 cm and weighs ≈500 gms. The system's capabilities to accommodate a removable μPC cartridge, perform multi-mode preconcentration, and inject in split or splitless mode are demonstrated. A μPC with micro-posts was coated with Tenax TA film to function as a test preconcentrator for the demonstration. The system was tested under laboratory conditions using a synthetic mixture. The system performance was further assessed using ambient air samples from various locations. The results were contrasted with the sorbent tube sampling technique followed by thermal desorption and injection into the GC-MS system using a TDU. Table 1 compares FEMI-AS with existing sample processing techniques and highlights the features, advantages, and disadvantages.

2. Materials and methods

2.1. Materials

Silicon wafers (4 in. dia., 1000 μm thick, double side polished) and

Borofloat wafers (4 in. dia. 500 μm thick, double side polished) were sourced from University Wafers (MA, USA). Platinum and titanium were obtained from Kurt J. Lesker (PA, USA). AZ 10XT photoresist was purchased from Micro-chemicals (Ulm, Germany). Tenax TA (80/100 mesh) and all chemicals used for chromatographic characterization were of analytical standard (>99% purity) and purchased from Sigma-Aldrich (MO, USA). Polymicro capillary tubing (ID 320 μm, OD 450 μm, TSP320450), double action spring contacts (0880-1-15-20-82-14-11-0), and DC fans (CFM-4010B-080–296) were acquired from Mouser (TX, USA). GC septum (27082) and separation column (13638–124) were purchased from Restek (PA, USA). Fused silica fittings (ZX1PK) and reducing ferrules (FS1·5 PK) were acquired from VICI (TX, USA). The diaphragm pump (E161-11-50), latching valves (LHLA0521211H), and metering valves (EW-02013-90) were sourced from Parker Hannifin (USA), The Lee Company (USA), and Idex (USA), respectively. Resins (Rigid 4000 resin and High Temp resin) for SLA 3D printing were purchased from Formlabs (MA, USA).

2.2. Micropreconcentrator design and fabrication

The micropreconcentrator architecture with micro-posts and multiple inlets/outlets has been discussed in detail in our previous publications [54]. Previous work investigated different micro-post designs and noted that a capsule shape with a staggered arrangement design for micro-posts and multiple inlets/outlets resulted in improved flow distribution and total internal surface area. For this study, the μPC was redesigned to have a larger sample capacity and better flow characteristics. The redesigned μPC is a 17 mm × 29 mm silicon-glass chip with 23,000 teardrop-shaped micro-posts inside its 15 mm × 15 mm square cavity (Fig. 2) compared to 3,500 micro-posts in the previous work. The current design has a total inner surface area of 3,200 mm^2 and a total internal volume of 90 μL compared to 200 mm^2 and 6.5 μL in the older designs. Teardrop-shaped micro-post and tapered inlets/outlets reduced the back pressure by 65% compared to older devices with capsule-shaped micro-posts with right-angled inlets/outlets (Fig. 2A).

The fabrication process of the μPC is similar to that of the MEMS separation column described in detail in our previous publications [55] and is illustrated in Fig. 2C. The devices with high aspect ratio features were realized by etching a 1,000 μm-thick silicon wafer to an etch depth of 500 μm using a deep reactive ion etching process followed by anodic bonding of a 500 μm-thick Borofloat wafer. A ≈400 nm thick plasma enhanced chemical vapor deposition (PECVD) oxide was deposited on the backside to act as an electrical insulator. A 30/300 nm Ti/Pt film stack was deposited using physical vapor deposition (PVD) and patterned using lift-off to form on-chip heaters and temperature sensors (Fig. 2D). After wafer dicing; individual chips were coated with 10 mg/mL Tenax TA adsorbent solution, similar to MEMS separation column functionalization described in our previous publications [56,57]. See appendix section A.1.1 for a summary of the coating process. A purpose-built FEMI-inspired μPC manifold (Fig. A1) was used to attach long capillary tubing for coating and conditioning individual chips. The chips were conditioned at 230 °C for >2 h with a continuous helium flow. The capillary tubing was discarded to avoid any sample loss and sample accumulation in transfer lines during use, and the conditioned preconcentrator was packaged and stored in a FEMI-μPC cartridge-plug assembly until needed.

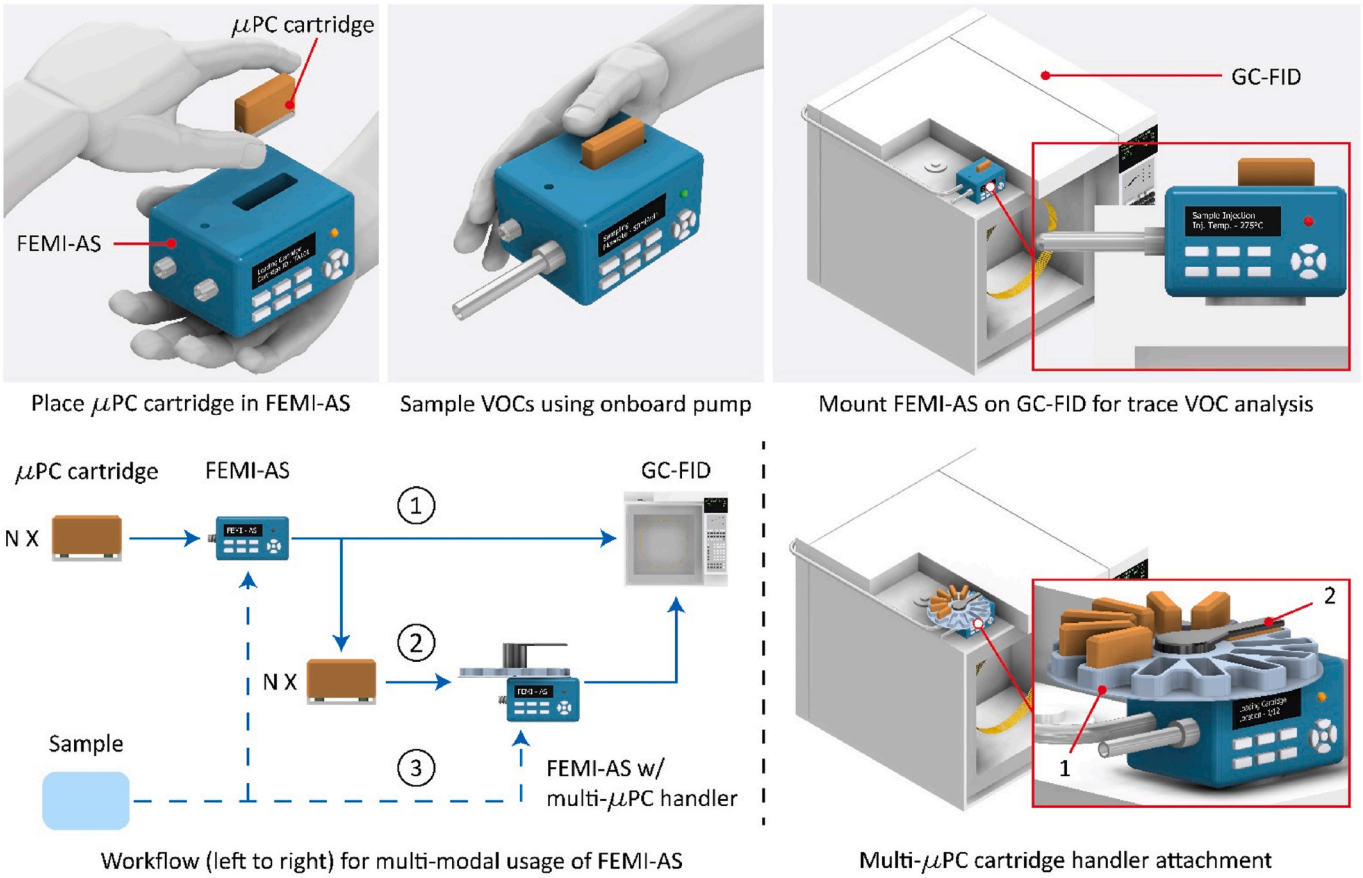

Fig. 1. FEMI-AS concept. (Top) Steps to use FEMI-AS as direct in-situ preconcentrator followed by off-site desorption and injection for analysis using GC-FID. (Bottom left) Workflow to use FEMI-AS as direct in-situ preconcentrator (1), multi-chip in-situ preconcentrator and injector (2), and off-site preconcentrator (3). (Bottom right) multi-μPC cartridge handler attachment with motorized cartridge tray (1) and loading arm (2) for unattended system operation.

2.3. Fluidic and Electrical Modular Interfacing (FEMI) architecture

In patent-pending FEMI architecture, removable electrical connections between microfabricated components and external electronics are established using double-action spring contacts and an interfacing PCB. Gas-tight, removable fluidic connections are created with the help of a Polymicro capillary tube (L < 2 cm) as an interfacing conduit between two fluidic components. A high-temperature GC septum is coaxially attached to the capillary tube, leaving at least 2.5 mm of the capillary tube on one side of the septum to act as the sealing element. The first-generation FEMI architecture (Fig. 3) consists of two key components: a) a FEMI bracket and b) a FEMI chip cartridge. For the FEMI-AS prototype, a 3D printed (Rigid 4000 resin) FEMI bracket is designed to hold two 2 cm long capillary tubes with the septum attached at predetermined locations that align with μPC inlet and outlet. The FEMI bracket and an interfacing PCB (Fig. 3A) are attached to the FEMI-AS chassis to form a μPC cartridge receiver with fluidic and electrical interconnects.

The 3D printed (High Temp resin) FEMI-μPC cartridge (Fig. 3B), consisting of multiple double-action spring contacts, a chip holder, and a pin holder, is designed to house the μPC chip. The pin holder secures individual double-action spring contacts. When mounted, the chip holder is designed to easily align μPC inlets and outlets with capillary tubes on the FEMI bracket. During mounting, the septum ends of the capillary tubes on the FEMI bracket are easily inserted into μPC fluidic ports. The attached GC septum is pressed against the sidewall of the μPC by fastening the FEMI bracket and μPC cartridge together using two M3 screws. The compressed septum (Fig. 3C inset) forms a removable gas-tight seal around the μPC fluidic ports, while spring contacts form electrical connections between μPC and interfacing PCB. The long ends of the capillary tubes are connected to fused silica fittings using reducing ferrules for system integration. Alternatively, the FEMI bracket alone can hold GC septa without a capillary tube attached to it to act as a plug to store functionalized preconcentrators.

2.4. FEMI-AS design and system integration

The first-generation FEMI-AS, along with a removable FEMI-μPC cartridge, works as a single-stage sample preconcentration and thermal desorption unit to eliminate the need for re-focusing. It is designed to sit on top of the GC injection port to reduce dead volume and eliminate the need for heated transfer lines between FEMI-AS and the separation column during analysis. Fig. 4 presents FEMI-AS integration with a conventional GC-FID system (7890A, Agilent, USA). The small size (Fig. 4A) compared to Agilent Autoinjector (G4513A, Agilent, USA) and onboard electronics allows FEMI-AS to operate as a standalone sample collector-preconcentrator for direct in-situ sampling and as a GC-integrated preconcentrator for off-site preconcentration.

For direct in-situ preconcentration, FEMI-AS is equipped with a conditioned FEMI-μPC cartridge and is used as a standalone in-situ sample preconcentrator before mounting on the GC-FID for off-site sample desorption and analysis. For off-site preconcentration (Fig. 4B), FEMI-AS is mounted on the GC and is loaded with a pre-conditioned FEMI- μPC cartridge to function as an off-site sample preconcentrator for samples collected using Tedlar bags. For analysis, an external high-purity carrier gas line is attached to the system, and the carrier gas required for sample injection and separation is provided through FEMI-AS. In this study, the carrier gas to FEMI-AS was supplied using the secondary GC inlet (GC Inlet B) for precise flow control during injection and separation. The primary GC inlet (GC Inlet A) pressure is disabled, and the inlet temperature is set to elevated temperatures to avoid condensation during sample injection. The separation column is sent through the disabled GC inlet port liner for sample injection and separation and is connected to the PEEK cross-connector included in FEMI-AS (Fig. 4C). The FEMI-AS prototype uses a screw fastening mechanism (Fig. 4E) to replace μPC cartridges for operation in various modes.

A highly programmable Python-based Graphical User Interface (GUI) and a highly modular embedded platform were developed in-house to build and program various micro-Total Analysis Systems (μTAS). Our previous publication describes the software and hardware implementations in great detail [58]. This study used the GUI to program the valve and pump states associated with different steps in FEMI-AS operation (Fig. A2). It also allows for complex temperature programming profiles for μPC use in selective preconcentration and injection applications. This is possible using in-built PWM (Pulse Width Modulation) signals and PID (Proportional, Integral, Derivative) temperature control algorithms. The microcontroller (TM4C1294NCPDT, Texas Instruments, Texas, USA) based embedded platform communicates with the GUI using Wi-Fi to download the user-generated program that drives various hardware layers and executes the program.

Table 1
FEMI-AS comparison with existing literature.

	Sorbent tubes [38–42]	Field deployable Thermal desorption unit [43]	Micropreconcentrators [29,53]	FEMI-AS w/ 3D printed μPC cartridge (This study)
Device architecture	Stainless steel or glass tube packed with an adsorbent	Purpose-built glass tubes filled with adsorbent	Microfabricated cavity filled with adsorbent or cavity with adsorbent coating on embedded pillars	Microfabricated cavity with adsorbent coating on embedded pillars packaged as a swappable 3D printed cartridge
Sampling and injection	Two-stage sampling (sorbent tube + cold trap). It uses TDUs for desorption and GC for split/splitless injection.	Single-stage sampling. It uses onboard heaters for desorption, and GC split control for split/splitless injection.	Single-stage sampling. It uses on-chip heaters for desorption and external components for split injection control.	Single-stage sampling. It uses on-chip heaters for desorption and has onboard split/splitless injection control.
Injection plug width	0.80–3.5 s	≈5 s	0.35 s	0.24 s
Peak area RSD%	5–20%	35–50%	<5%	≈10%
Sampling cond.	5–30 min at 10–80 ml/min	6 min at 80 ml/min	10–30 min at 1–10 ml/min	20 min at 50–75 ml/min
LOD	2 pg/L to 5 ng/L	n.a.	≈100 pg/L to 50 ng/L	12 pg/L to 8 ng/L
Size, Weight, and Power	62 cm × 38 cm X 55 cm, 32 Kgs, 900 W (TD100-xr)	12.5 cm × 17 cm X 20 cm (concept only)	No existing system	9.5 cm × 10 cm X 20 cm, 0.5 Kgs, 30 W
Advantages	Highly integrated with GCs and have large sample capacities and a broad range of adsorbents. Sorbent tubes are relatively inexpensive	Suitable for in-situ analysis, has large sample capacities and a broad range of adsorbents	Suitable for in-situ analysis and a wide range of applications. Have very low power consumption. Inexpensive when produced at scale.	Suitable for in-situ analysis and a wide range of applications. It Has very low power consumption. Very easy to integrate with all GCs. Inexpensive.
Disadvantages	TDU is very expensive and power-hungry. Not suitable for in-situ analysis and a full range of applications	Cons: Not suitable for a broader range of applications	Cons: low dynamic range. They need a cleanroom for fabrication. Hard to integrate with GCs	Cons: low dynamic range. It requires a cleanroom for fabrication.

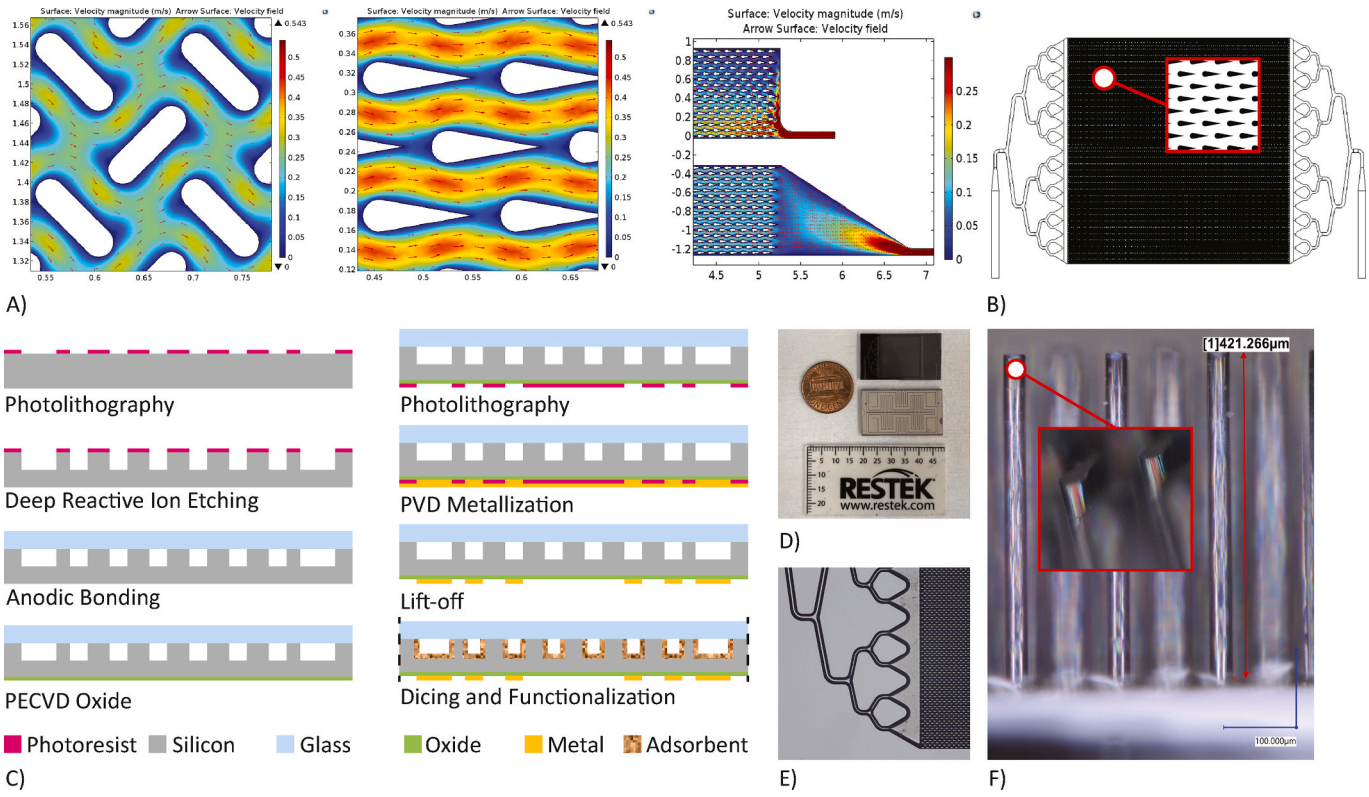

Fig. 2. Design and fabrication of micropreconcentrators. A) CFD simulation of flow velocity in the teardrop-shaped micro-posts (compared to capsule-shaped micro-posts) in a cavity with tapered inlets/outlets. B) Multi-inlet preconcentrator design with teardrop micro-posts. C) Fabrication process flow. D) µPC with on-chip heater and temperature sensor. E) Etched inlets with teardrop micro-post. F) Etching of high aspect ratio micro-posts using DRIE.

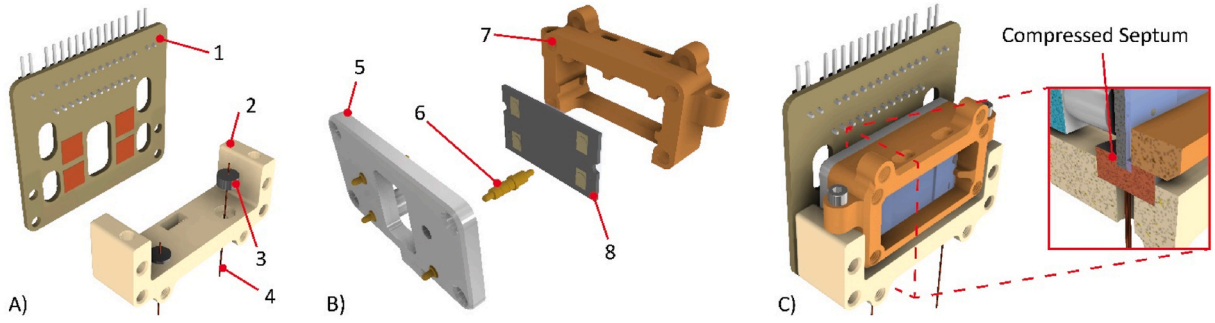

Fig. 3. First-generation FEMI architecture. A) FEMI receiver with interfacing PCB (1), FEMI bracket (2), GC septum (3), Polymicro capillary tube (4). B) FEMI chip cartridge consisting of pin holder (5), double-action spring contacts (6), chip holder (7), and micropreconcentrator (8). C) Cartridge and bracket assembly using a screw mechanism.

2.5. System operation

FEMI-AS (Fig. 5A) generally operates in four steps: 1) Sample collection and preconcentration of trace analytes at desired temperatures; 2) Desorption of analytes at high temperatures; 3) Split/Splitless sample injection into the GC separation column, and 4) Sample separation at programmed flow rates and temperatures. FEMI-AS implements sampling flow through the micropreconcentrator in the opposite direction compared to injection and sample separation flow allowing for reverse temperature programming of multi-bed micropreconcentrators when needed. For this study, the micropreconcentrators were sampled at room temperature. Sampling was performed using an onboard diaphragm pump connected to the 'NV1' metering valve for sampling flow rate control. The flow rate was set to 50 mL/min, and the sampling time varied from 2 s to 1,200 s. The sampling flow path (Fig. 5B) was determined using latching valves included in FEMI-AS. During the thermal desorption cycle (Fig. 5C), the valve states were programmed to ensure no gas flow through the preconcentrator. A PWM power (≈30 W DC) was supplied to the on-chip heater to reach a maximum of 275 °C at an average heating rate of 10 °C/s (600 °C/min). The preconcentrator was held at 275 °C for at least 5 s to ensure complete desorption of analytes.

After a 5-s hold time, valve 'V1' was switched to inject the desorbed sample into the separation column (Fig. 5D). Valve 'V3' determines the split/splitless injection, and the split ratio was manually adjusted using a metering valve 'NV2'. The split ratio was pre-calibrated for the attached column, and the split flow rate (i_{Split}) was measured using an external flow meter (ADM 1000, Agilent, USA) to program split ratios between runs. The calibration process and the total flow rate through the µPC ($i_{\mu PC}$) at different split ratios are detailed in Appendix A.1.3. Injection plug widths as short as 240 ms were observed, alleviating the need for a re-focusing step. A DC fan was programmed to cool the preconcentrator

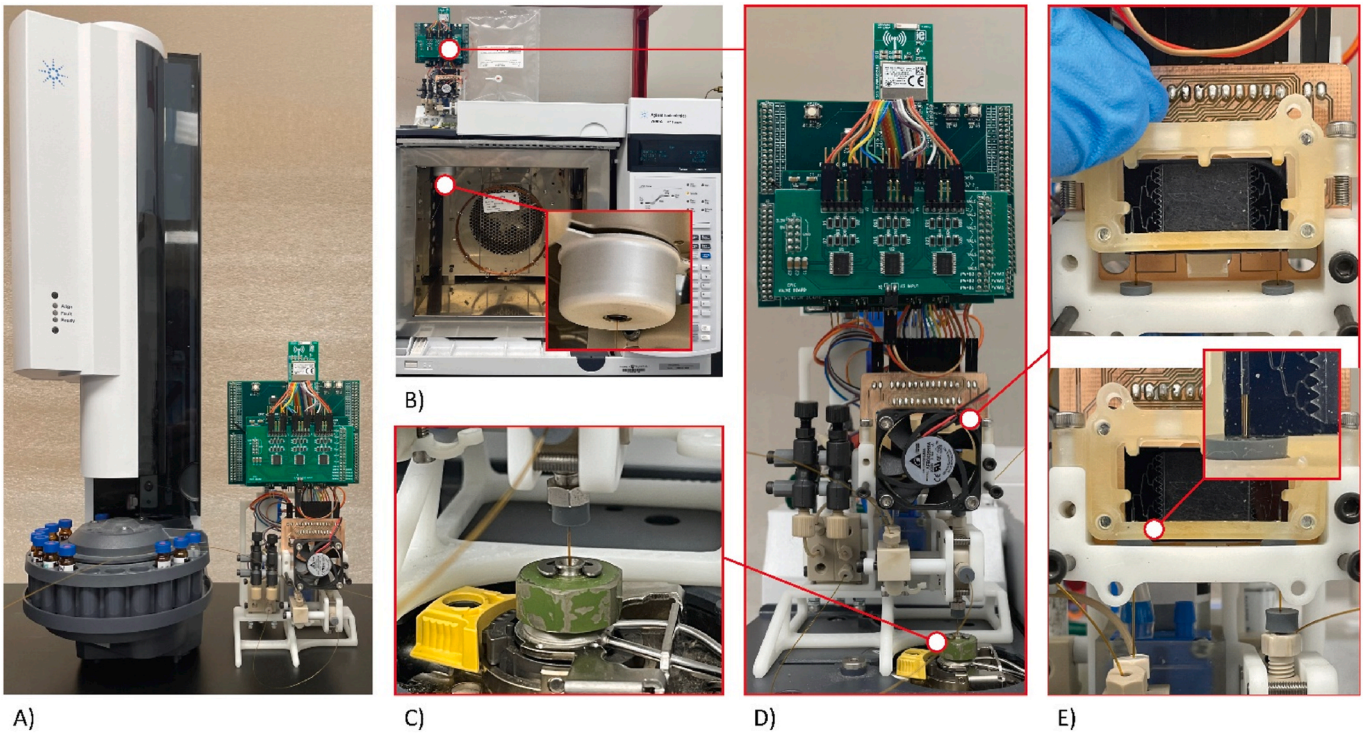

Fig. 4. FEMI-AS implementation and integration with Agilent GC-FID. A) Size comparison with Agilent Autoinjector and FEMI-AS usage in in-situ preconcentrator mode. B) FEMI-AS mounted on GC-FID for off-site preconcentrator mode and VOC analysis. C) Fluidic Interface between FEMI-AS and separation column. D) Fully assembled FEMI-AS with onboard electronics. E) μPC cartridge installation.

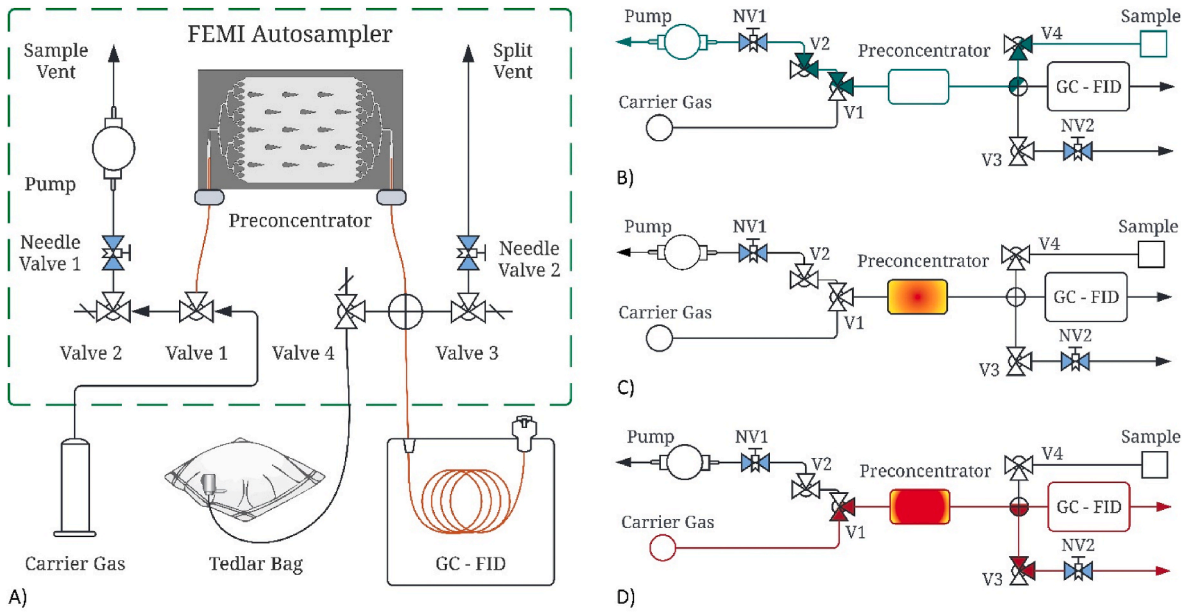

Fig. 5. System schematic and operation. A) FEMI-AS fluidic components and Integration with GC-FID B) Sampling (flow path in green). C) Desorption (no flow). D) Split injection and separation (flow path in red). (For interpretation of the references to colour in this figure legend, the reader is referred to the Web version of this article.)

down to room temperature immediately after injection.

The valve states were programmed for separation with an optional gas-saver mode where valve 'V3' blocks the split flow through 'NV2'. The temperature programming for the separation stage was accomplished using the GC oven. The GC inlet used for the carrier gas supply (GC Inlet B) was set to constant pressure during the injection. Depending on the experiment, the inlet was switched to a "constant flow rate" setting during the separation stage. This was done to maintain a constant flow rate through the separation column during temperature ramping to match GC-MS operation. The valve states in FEMI-AS were time-synchronized with GC inlet and oven settings to achieve proper function. In future work, a flow controller for carrier gas supply and proportional valves for sampling flow rate and split control will be incorporated into FEMI-AS for complete fluid flow automation.

2.6. Experimental conditions

2.6.1. Gas samples

The preconcentration and split/splitless injection performance were characterized using a 15-compound synthetic mixture including alkanes, aromatic halides, aromatic hydrocarbons, and nitro-aromatics. These compounds reflect some of the VOCs present in environmental samples, and the complete list of compounds with boiling points is listed in Table 2. As a first step in preparing the trace-level gas sample, equal liquid volumes (100 μL) of each of the 15 compounds were combined in an autosampler vial (2 mL). This liquid mixture was used as a starting solution for subsequent volumetric dilution in the gas phase. A "25-ppb" gas sample with an average gas phase analyte concentration of 25 ppb was prepared in a 1 L Tedlar bag filled with helium by injecting 2 nL of this liquid mixture. A 2 nL liquid volume was achieved indirectly by injecting 0.2 μL of the solution into the Tedlar bag with a split ratio of 100:1 using an Agilent Autoinjector (G4513A, Agilent, USA). The resultant sample had analyte concentrations ranging from 14 ppb (dodecane) to 30 ppb (toluene), and the estimated concentrations for all compounds are listed in Table 2. Lastly, as environmental gas samples, the ambient air surrounding the lab's chemical storage cabinet and from the building hallway was sampled by direct in-situ preconcentration using FEMI-AS and sorbent tubes for FEMI-AS comparison with TD-GC-MS.

2.6.2. Sampling and analysis

For split/splitless injection characterization, the vial with the 15-compound liquid mixture was held close to the sampling inlet and was opened. The ambient air surrounding the vial's opening was sampled instead of the headspace of the vial. This was done to avoid overloading valves and PEEK connectors in the system while ensuring adequate capture of analytes on the preconcentrator for injection with large split ratios. After sampling for 2 s at 50 mL/min, the analytes were desorbed and injected into GC-FID with different split ratio settings. Similarly, for preconcentration characterization, the "25-ppb" sample Tedlar bag was connected to the FEMI-AS inlet using capillary tubing (Fig. 4B) and sampled for 20 s at 50 mL/min. Also, a 25 cm long capillary tube (320 μm ID) was used in place of the μPC to act as a 20 μL sample loop for direct injection and for comparison with the μPC. After sampling, the analytes were desorbed and injected at a 1:1 split ratio. In both experiments, the samples were captured at room temperature and desorbed at 275 °C. The carrier gas pressure was set to 15 psi in constant pressure mode for both injection and separation. Gas saver mode on FEMI-AS was used after injection to limit carrier gas consumption.

FEMI-AS was compared to TD-GC-MS (TD100-xr, Markes International and FocusGC DSQ II, Thermo Fisher) for analysis of environmental samples. The separation column flow rate was adjusted on the FEMI-AS system using C7–C30 saturated alkanes to match retention times generated by GC-FID with those generated by GC-MS. This was done to help identify analytes in ambient air based on retention times obtained using FEMI-AS coupled with GC-FID. Additionally, the TD-GC-MS response for a known concentration of alkanes was calibrated (appendix section A.1.4) to help estimate the alkane concentrations in environmental samples. For analysis using TD-GC-MS, a stainless-steel sorbent tube was packed with Tenax TA and attached to a portable sampling pump. The FEMI-AS and the sorbent tube sampler were moved from location to location to sample ambient air. First, the ambient air from different areas was captured for 20 min at a 50 mL/min sampling flow rate. After sampling, the FEMI-AS was mounted on GC-FID, and the sorbent tube was loaded into the TD system for analysis using GC-FID and GC-MS, respectively. While FEMI-AS performed a single-stage desorption and injection at a 5:1 split ratio in <1 min, the TD system desorbed the analytes at 275 °C for 8 min and transferred the analytes onto a cold trap maintained at −30 °C for a second stage focusing. The analytes in the cold trap were desorbed at 320 °C for 5 min and were injected into GC-MS with a 5:1 split. The operating parameters for sample separation using GC-FID and GC-MS for all experiments are described in Table 3.

Table 2
Compounds in synthetic mixture with boiling points and individual concentrations in a "25-ppb" gas sample.

Peak No.	Compound	Boiling Point (°C)	Concentration (ppb)
1	Heptane	98.4	22.1
2	Octane	125.6	19.9
3	Nonane	151	18.1
4	Toluene	110.6	30.4
5	p-Xylene	138.4	26.2
6	m-Xylene	139	26.3
7	o-Xylene	144	26.8
8	Dodecane	216	14.2
9	Chlorobenzene	131.6	31.9
10	Isobutylbenzene	173	20.6
11	1,2 - Dichlorobenzene	180	28.7
12	Benzyl chloride	179	28.4
13	1,2,4 - Trichlorobenzene	214	25.9
14	2-Nitrotoluene	222	27.4
15	3-Nitrotoluene	231	27.3

3. Results and discussion

3.1. Fluidic interfacing

The removable fluidic interfacing for the μPC is designed to provide inert, leak-free connections and sustain high gas pressures during operation at elevated temperatures. The FEMI connections were tested for reliability by connecting 20 cm long capillary tubes to the μPC inlet and outlet using a FEMI cartridge. Initially, the outlet was sealed using a PEEK plug, and the inlet was connected to a helium gas source to check for maximum holding pressure. The assembly was submerged in an 80 °C water bath, and the inlet pressure was gradually increased from 5

Table 3
Analytical settings for GC-FID and TD-GC-MS for different experiments.

Experiment	Instrument	Parameter	Value/State
Split/Splitless Injection peak resolution Trace-level synthetic mixture sampling	FEMI-AS GC-FID (Agilent 7890A)	Column	SGE BP20 (15 m × 0.22 mm ID X 0.25 μm film thickness)
		Inlet mode	Constant pressure
		Inlet pressure	15 psi
		Gas saver mode	On
		Oven program	Step 1: 60 °C for 3 min Step 2: 120 °C/min to 180 °C Step 3: 180 °C for 3 min
Environmental sampling	FEMI-AS GC-FID (Agilent 7890A) TD (TD100-xr) GC-MS (FocusGC - DSQ II)	Column	Rxi-5Sil (30 m × 0.25 mm ID X 0.5 μm film thickness)
		Inlet mode	Constant flow
		Inlet flow rate	1 mL/min (GC-MS); 1.75 mL/min (GC-FID)
		Gas saver mode	On
		Oven program	Step 1: 40 °C for 1 min Step 2: 10 °C/min to 180 °C Step 3: 180 °C for 1 min
		Total ion chromatogram (TIC) mode	35–350 *m/z*

to 30 psi. The cartridge showed no signs of leakage within the operating pressure range. Next, the flow rate through FEMI μPC cartridge at different inlet pressures was measured in the same setup. The results were compared to a μPC with permanent capillary connections created using adhesives. Fig. A4 shows the flow response at different pressures with a maximum flow rate of 410 mL/min at 30 psi and a <4% variation compared to permanent connections.

To test for inertness, baseline experiments for devices with FEMI and permanent connections were conducted using unfunctionalized μPCs and GC-FID. The inlet of the μPC was connected to the GC inlet and the outlet to FID. With carrier gas flowing through the devices, the GC oven temperature was raised to 230 °C and held for >2 h to imitate the μPC conditioning step. The observed baseline shift was similar in both connections and was less than 2 pA at 230 °C. Also, the baseline was stable at 230 °C, indicating a leak-free steady flow through the preconcentrators with FEMI connections. Notably, the fluidic connections on FEMI-AS sustained more than 100 thermal cycles with temperatures reaching 275 °C for short durations without needing replacement. The reliability was further tested by connecting the μPC cartridge to GC-FID and estimating the relative standard deviation (RSD%) of μPC desorption peak areas. 0.1 μL dodecane (liquid) was injected five times into the μPC using a GC autoinjector. The analyte not retained by the adsorbent bed during each injection appeared as a breakthrough peak. After five consecutive injections, an 18 V DC was manually applied across the on-chip heater for desorption at 250–280 °C. The desorption peak areas were repeatable with an RSD% of less than 22% (Fig. A5). Most of the variation is due to experimental errors in the autoinjector's liquid injection volume and desorption temperature control, with an RSD% of 7.5% and 6%, respectively. With around 10% error in peak areas due to the FEMI-μPC cartridge, the described FEMI connections are suitable for repeated and extended use at high temperatures in GC applications.

3.2. Split/splitless injection peak resolution

A split injection technique for high-concentration analytes has been widely used to mitigate overloading effects in capillary and MEMS separation columns. On the other hand, a splitless injection is necessary for low-concentration analytes to meet the LOD. Therefore, a split/splitless injection is a crucial function of any GC injection system. Peak-resolution experiments were conducted using the synthetic mixture to test the split/splitless injection functionality of FEMI-AS. Gaussian peak resolution (R_G) and peak separation factor (α) were estimated as indicators for peak resolution. The Gaussian peak resolution is defined as $R_G = 1.18\ (Rt_2 - Rt_1)/(W_{0.5h,2} + W_{0.5h,1})$, where Rt_1, Rt_2 are retention times and $W_{0.5h,1}$, $W_{0.5h,2}$ are peak widths at half height of successive peaks. The separation factor is defined as $\alpha = (Rt_2 - Rt_0)/(Rt_1 - Rt_0)$, where Rt_0 is the retention time of the unretained analyte. A sharper injection plug width ($W_{0.5h,\ i}$) and a more significant difference between retention times ($Rt_i - Rt_{i-1}$) result in higher peak resolution.

Fig. 6 compares the chromatographic peak separation using splitless injection and split injection with different split ratios. As expected, a splitless injection generated larger peaks due to the complete transfer of captured analytes. However, it suffers from wide injection plug widths, resulting in reduced peak resolution due to a reduced injection flow rate. Broadened peaks resulted from the coelution of closely eluting xylene isomers (peaks 5 and 6). With a split injection, a fraction of captured analytes was transferred into the GC column, but the xylene isomers were separated. As shown in Table 4, the reduced plug width ($W_{0.5h}$) and increased peak resolution (R_G) with a rising split ratio reflect the better separation of the xylene isomers. The improved plug width and peak resolution can be attributed to the increased total flow rate through the μPC ($i_{\mu PC}$) from 3.3 mL/min in splitless injection to 71 mL/min in 100:1 split injection. These observations align with previous literature [59].

However, the separation factor (α) decreases with an increasing split ratio. The shift in retention times and reduction in α is due to changing flow rates during sample separation caused by the basic implementation of gas-saver mode and lack of flow control through the column during temperature programming. Therefore, automating flow control in next-generation FEMI-AS would be crucial. It is worth noting that dodecane was not detected, and the peaks for 1,2,4 – trichlorobenzene, 2-

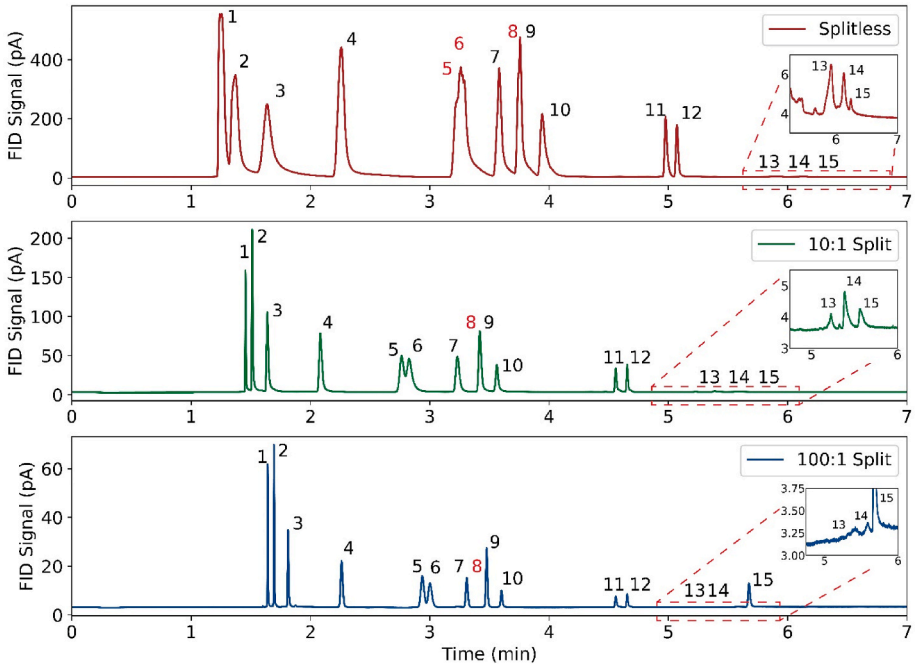

Fig. 6. Effect of split ratio on chromatographic resolution demonstrated using a complex mixture. Peak numbers in red indicate a missing peak or that a clearly resolved peak was not evident for the compound. (For interpretation of the references to colour in this figure legend, the reader is referred to the Web version of this article.)

Table 4
Plug width, peak resolution, and separation factor of Xylene Isomers.

	$W_{0.5h}$ (s)				R_G				α			
	Splitless	1:1	10:1	100:1	Splitless	1:1	10:1	100:1	Splitless	1:1	10:1	100:1
Heptane	2.76	0.64	0.49	0.39	–	–	–	–	–	–	–	–
p-Xylene	4.78	2.77	2.256	1.81	8.3	9.19	12.76	16.05	1.62	1.68	1.64	1.55
m-Xylene	4.78	3.83	2.826	2.02	0	0.59	0.89	1.20	1	1.03	1.03	1.03
o-Xylene	2.42	3.34	2.16	1.146	3.16	4.32	5.74	6.87	1.12	1.27	1.22	1.15

nitrotoluene, and 3-nitrotoluene were small. This can be attributed to the high boiling points of each of these compounds and their relatively low concentration in the vial's headspace at room temperature [60] and, consequently, in the sampled ambient air. The retention times and estimated peak resolution indicators for the first 12 compounds are listed in Table A3.

3.3. Trace-level synthetic mixture sampling

To demonstrate the functionality of the FEMI-AS system as an off-site preconcentrator, a Tedlar bag containing a "25-ppb" synthetic sample (Table 2) was sampled for 20 s at 50 mL/min using the μPC and a 20 μL sample loop, and the captured analytes were analyzed using GC-FID (Table 3). Fig. 7 shows the relative chromatographic responses for 1:1 split injection using the μPC and the sample loop. As observed, FEMI-AS equipped with the μPC captured almost all the analytes (except dodecane) compared to the one with the sample loop. However, a slightly higher sampling flow rate of ≈75 mL/min enabled the detection of dodecane by processing a larger sample volume (25 mL), as shown in Fig. 7 inset. Also, a contaminant from Tedlar bags was detected using both the μPC and the sample loop, a well-reported problem of sample storage in polymer bags [61,62]. It was identified as N, N-dimethylacetamide using GC-MS. Although the GC-FID was programmed to have an aggressive temperature ramp rate of 120 °C/min, all the peaks are well-defined and separated.

Trace analysis using FEMI-AS and the μPC is significantly faster than the conventional TD-GC-MS technique. The total sample analysis time, including sampling, desorption, injection, and separation, was ≈8 min. Also, the ability to detect a ≈14 ppb analyte from a 25 mL sample in <8 min is equivalent to the field deployable thermal desorption system that uses custom-made sorbent tubes reported by Lecharlier et al. (2020) [43]. As the FEMI-μPC cartridge shows promising results, future work will focus on optimizing and characterizing the μPC design, adsorbents, and operating conditions for specific applications.

3.4. Environmental sampling

FEMI-AS, as an in-situ environmental preconcentrator, is demonstrated using ambient air samples from the building hallway and the area surrounding the lab's chemical storage cabinet. For semi-quantitative comparison, FEMI-AS and sorbent tubes containing Tenax TA sampled the air side-by-side for 20 min at 50 mL/min. The FEMI-AS samples were analyzed using GC-FID, and the sorbent tube samples were analyzed using TD-GC-MS. Fig. 8 shows chromatograms produced by both methods. As expected, the peak areas and heights were mostly smaller in the hallway sample compared to the chemical storage. While there are similarities between the two methods, FEMI-AS generated more peaks with retention times between 7 and 10 min (lower volatility compounds). In contrast, the sorbent tubes with TD-GC-MS produced more peaks with retention times between 1 and 6 min (higher volatility

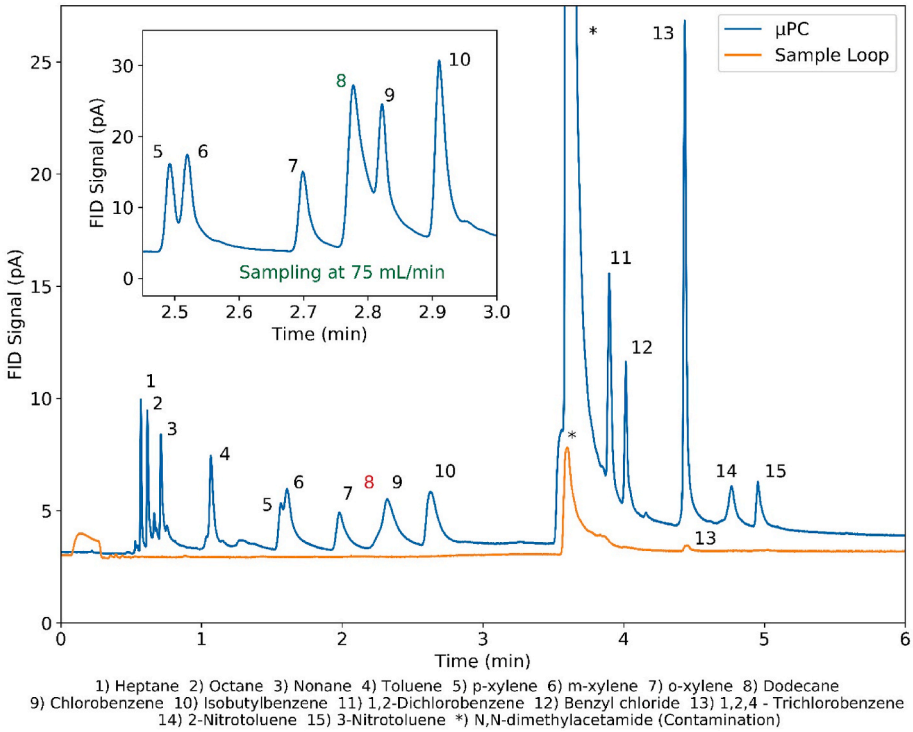

Fig. 7. Chromatographic response of FEMI-AS equipped with a μPC compared to FEMI-AS with a 20 μL sample loop for "25-ppb" samples collected at 50 mL/min and ≈75 mL/min (inset). Peak numbers in red and green indicate a missing and detected peak, respectively. (For interpretation of the references to colour in this figure legend, the reader is referred to the Web version of this article.)

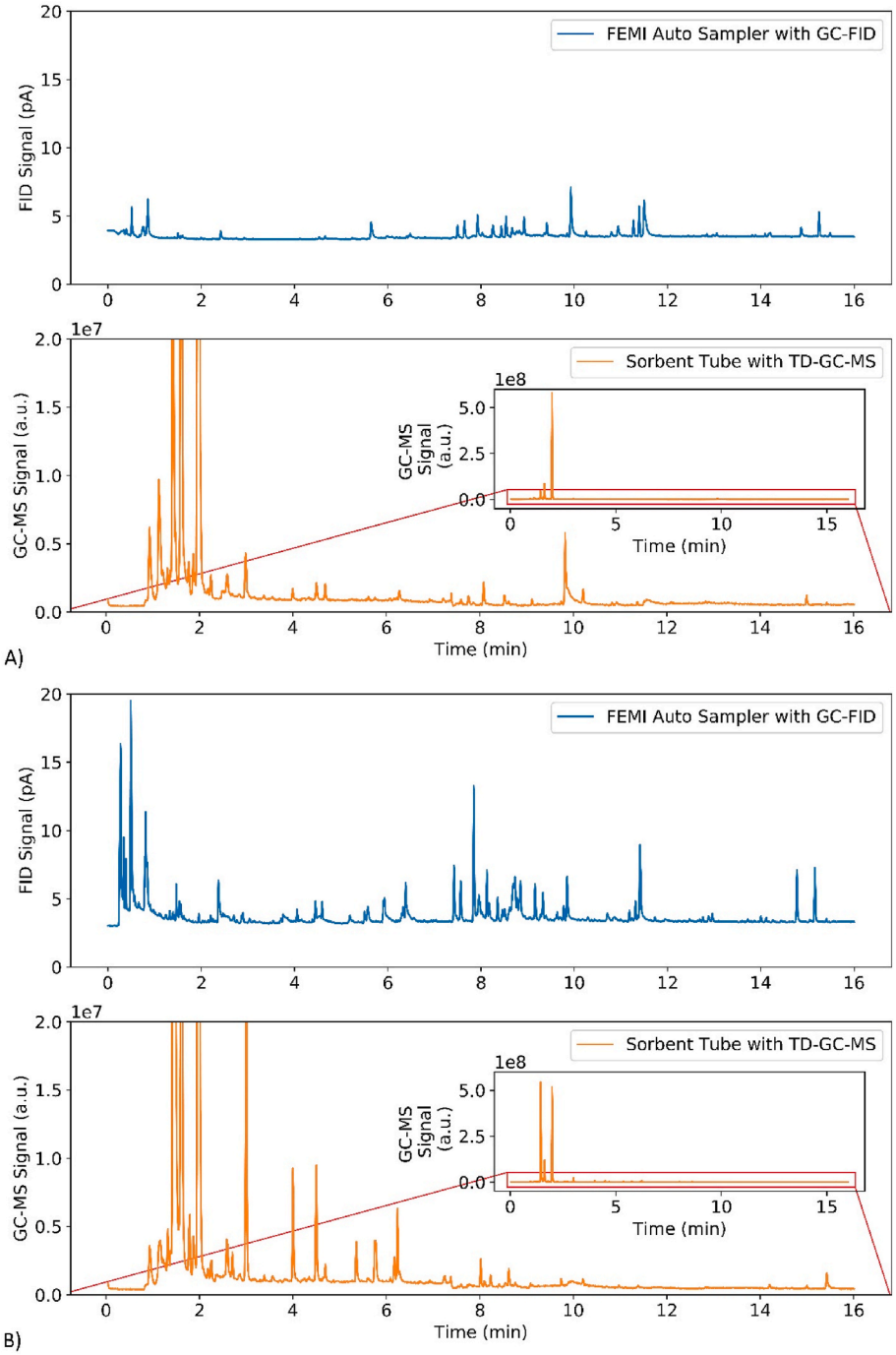

Fig. 8. Ambient air sampling using FEMI-AS and Sorbent tube. A) Air from the building hallway, B) Air surrounding the chemical storage cabinet.

compounds). A similar trend was observed with relative concentrations of analytes. As listed in Table A4 and A5, 21 compounds from the hallway and 33 compounds from the air near the chemical storage cabinet were identified using TD-GC-MS. Although more peaks were detected from FEMI-AS, 17 and 31 compounds were determined for the samples from the hallway and near the chemical storage cabinet, respectively, by comparing results from GC-FID with TD-GC-MS data. The estimated concentrations of analytes detected by FEMI-AS were <100 ppt. Based on these concentrations, the analytes' detection limits (LOD) were calculated using the signal-to-noise ratio approach [43,63]. LOD is generally defined as the analyte concentration when the instrument's signal-to-noise ratio (S/N) of the corresponding analyte is three. The signal-to-noise ratio is given as $S/N = H/\sigma$, where H is the peak height of the analyte from the baseline, and σ is the standard deviation (or noise) of the baseline signal. It is worth noting that adding FEMI-AS to FID did not change the baseline standard deviation significantly, and the σ for GC-FID with FEMI-AS was 0.12 pA. For a 20-min ambient air sampling, the LODs ranged from 0.002 ppb (12 pg/L) to 2 ppb (8 ng/L) (Table A4).

The difference in chromatographic outputs could be attributed to multiple factors. Conventional sorbent tubes have large sample capacities with adsorbent masses as high as 100 mg compared to 0.9 mg in the μPC. Their ≈6 cm long adsorbent bed allows for longer residence times for analytes to interact with adsorbents compared to the 15 mm square cavity in μPC used in this study. Different flow patterns through a packed sorbent tube vs. a field of teardrop-shaped micro-posts could also

contribute to contrasting results. Furthermore, TD-GC-MS uses a second-stage cold trap made of Carbopack B and Carbopack C, which is more suitable for high-volatility compounds (C4–C20) [64,65]. Also, multiple studies have shown that FID and MS detectors have different sensitivities and selectivities, with higher sensitivity in MS and higher selectivity in FID [66,67]. In the present form, FEMI-AS cannot be connected to GC-MS for a more direct comparison as the prototype lacks the precise flow control necessary to meet MS vacuum specifications. Future work will focus on incorporating flow control and integrating FEMI-AS with GC-MS. While a direct and fully quantitative comparison is currently not possible, this semi-quantitative comparison substantiates the FEMI-AS use for in-situ sample preconcentration of trace-analytes with sub-ppb concentrations.

4. Conclusion

The adoption of a microfabricated preconcentrator for broader applications has been stifled due to the lack of removable fluidic connections and thermal desorption units for micropreconcentrators to work with traditional gas chromatography systems. A novel modular fluidic and electrical interfacing (FEMI) between micropreconcentrators and analytical systems has been developed and described. A first-generation portable thermal desorption unit or autosampler (FEMI-AS) was constructed to integrate micropreconcentrators with gas chromatography systems for trace analysis. The inertness and reliability of the fluidic connections at temperatures as high as 230 °C were tested and proved compatible with gas chromatography applications. Split/Splitless injection and preconcentration functionality of FEMI-AS was characterized by sampling a 15-compound synthetic mixture and analyzing it using GC-FID. The system could generate sharp injection plugs (plug width ≈240 ms) and detect analytes with concentrations as low as 14 ppb within 20 s of sampling time and 8 min of analysis time. Ambient air samples were captured and analyzed using FEMI-AS, and the results were compared to conventional sorbent tube sampling and GC-MS analysis. The system detected a diverse set of analytes with concentrations <100 ppt.

The first-generation FEMI-AS demonstrated an easy and inexpensive method to incorporate a sampling and thermal desorption unit into conventional GCs for enhanced detection limits and extended functionality to analyze trace-level samples. The prototype established the detachable electrical connections and removable fluidic interfacing of microfabricated preconcentrators, ultimately empowering MEMS-based sample collection. This functionality significantly increased μPC development and integration flexibility by avoiding auxiliary and permanent side-port or top-port connections, often implemented to functionalize μPCs and interface μPCs with conventional components. The small size of the system with onboard sampling flow rate and split injection control supports cross-platform usability, such as portable GC and μGC.

The next generation will improve some of the deficiencies associated with the current design. For instance, the current system lacks the accurate flow control necessary for integration with GC-MS and constant flow rate programming in portable and μGC. Following the encouraging results, a second-generation FEMI-AS will be developed to incorporate automated flow control. The current cartridge design uses screws to establish leak-free fluidic connections. Although reliable, it is time-consuming and restricts automation. New cartridge latching mechanisms will be explored to enable faster cartridge installation. Due to material properties, the maximum operating temperature for FEMI-μPC cartridges is limited to 275 °C. New materials and fabrication techniques will be explored to extend the operating range to 350 °C. FEMI architecture will significantly reduce chip and system-level developmental complexities associated with device design, functionalization, characterization, and integration. This study lays the foundation for developing complex μTAS using FEMI architecture, and the development of FEMI-AS for micro-gas chromatography is in progress.

CRediT authorship contribution statement

Nipun Thamatam: Conceptualization, Methodology, Investigation, Formal analysis, Visualization, Writing – original draft, Writing – review & editing. **Jeonghyeon Ahn:** Methodology, Investigation, Formal analysis, Writing – original draft. **Mustahsin Chowdhury:** Software, Hardware, Writing – review & editing. **Arjun Sharma:** Software, Hardware. **Poonam Gupta:** Software, Hardware. **Linsey C. Marr:** Writing – review & editing, Supervision. **Leyla Nazhandali:** Writing – review & editing, Supervision. **Masoud Agah:** Conceptualization, Writing – review & editing, Project administration, Supervision.

Declaration of competing interest

The authors declare that they have no known competing financial interests or personal relationships that could have appeared to influence the work reported in this paper.

Data availability

Data will be made available on request.

Acknowledgments

This research has been supported by the National Institute for Occupational Safety and Health (NIOSH) under Award No. R01OH011350. The micropreconcentrators were fabricated at Virginia Tech's Micro and Nano Fabrication Laboratory (Micron) and the University of North Carolina's Chapel Hill Analytical and Nanofabrication Laboratory (CHANL).

Appendix A. Supplementary data

Supplementary data to this article can be found online at https://doi.org/10.1016/j.aca.2023.341209.

References

[1] R. Koppmann, Chemistry of volatile organic compounds in the atmosphere, Hydrocarbons, Oils and Lipids, in: Diversity, Origin, Chemistry and Fate, 2020, pp. 811–822.
[2] D.M. Pinto, J.D. Blande, S.R. Souza, A.-M. Nerg, J.K. Holopainen, Plant volatile organic compounds (VOCs) in ozone (O3) polluted atmospheres: the ecological effects, J. Chem. Ecol. 36 (2010) 22–34.
[3] P. Fink, Ecological functions of volatile organic compounds in aquatic systems, Mar. Freshw. Behav. Physiol. 40 (2007) 155–168.
[4] Y. Yang, L. Li, Total volatile organic compound emission evaluation and control for stereolithography additive manufacturing process, J. Clean. Prod. 170 (2018) 1268–1278.
[5] P. Azimi, D. Zhao, C. Pouzet, N.E. Crain, B. Stephens, Emissions of ultrafine particles and volatile organic compounds from commercially available desktop three-dimensional printers with multiple filaments, Environ. Sci. Technol. 50 (2016) 1260–1268.
[6] H. Wang, L. Nie, J. Li, Y. Wang, G. Wang, J. Wang, et al., Characterization and assessment of volatile organic compounds (VOCs) emissions from typical industries, Chin. Sci. Bull. 58 (2013) 724–730.
[7] H. Bouwmeester, R.C. Schuurink, P.M. Bleeker, F. Schiestl, The role of volatiles in plant communication, Plant J. 100 (2019) 892–907.
[8] J. Peñuelas, J. Llusià, Plant VOC emissions: making use of the unavoidable, Trends Ecol. Evol. 19 (2004) 402–404.
[9] J. Kesselmeier, M. Staudt, Biogenic volatile organic compounds (VOC): an overview on emission, physiology and ecology, J. Atmos. Chem. 33 (1999) 23–88.
[10] F. Loreto, S. Fares, Biogenic volatile organic compounds and their impacts on biosphere–atmosphere interactions, Dev. Environ. Sci. 13 (2013) 57–75.
[11] M. Rissanen, Anthropogenic volatile organic compound (AVOC) autoxidation as a source of highly oxygenated organic molecules (HOM), J. Phys. Chem. 125 (2021) 9027–9039.
[12] P. Wolkoff, Volatile organic compounds, Indoor Air 3 (1995) 1–73.
[13] H. Rajabi, M.H. Mosleh, P. Mandal, A. Lea-Langton, M. Sedighi, Emissions of volatile organic compounds from crude oil processing–Global emission inventory and environmental release, Sci. Total Environ. 727 (2020), 138654.
[14] A.J. Li, V.K. Pal, K. Kannan, A review of environmental occurrence, toxicity, biotransformation and biomonitoring of volatile organic compounds, J. Environ. Chem. Ecotoxicol. 3 (2021) 91–116.

[15] V. Soni, P. Singh, V. Shree, V. Goel, Effects of VOCs on Human Health, in: N. Sharma, A. Agarwal, P. Eastwood, T. Gupta, A. Singh (Eds.), Air Pollution and Control. Energy, Environment, and Sustainability, Springer, Singapore, 2018. https://doi.org/10.1007/978-981-10-7185-0_8.

[16] M. Kampa, E. Castanas, Human health effects of air pollution, Environ. Pollut. 151 (2008) 362–367.

[17] Z. Li, R. Paul, T. Ba Tis, A.C. Saville, J.C. Hansel, T. Yu, et al., Non-invasive plant disease diagnostics enabled by smartphone-based fingerprinting of leaf volatiles, Nat. Plant 5 (2019) 856–866.

[18] G. Buchbauer, F. Buljubasic, The scent of human diseases: a review on specific volatile organic compounds as diagnostic biomarkers, Flavour Fragr. J. 30 (2015) 5–25, https://doi.org/10.1002/ffj.3219.

[19] A.D. Wilson, Applications of electronic-nose technologies for noninvasive early detection of plant, animal and human diseases, Chemosensors 6 (2018) 45.

[20] I.A. Ratiu, T. Ligor, V. Bocos-Bintintan, C.A. Mayhew, B. Buszewski, Volatile organic compounds in exhaled breath as fingerprints of lung cancer, asthma and COPD, J. Clin. Med. 10 (2020) 32.

[21] L.D. Bos, P.J. Sterk, S.J. Fowler, Breathomics in the setting of asthma and chronic obstructive pulmonary disease, J. Allergy Clin. Immunol. 138 (2016) 970–976.

[22] M. Phillips, R.N. Cataneo, B.A. Ditkoff, P. Fisher, J. Greenberg, R. Gunawardena, et al., Volatile markers of breast cancer in the breath, Breast J. 9 (2003) 184–191.

[23] S. Grassin-Delyle, C. Roquencourt, P. Moine, G. Saffroy, S. Carn, N. Heming, et al., Metabolomics of exhaled breath in critically ill COVID-19 patients: a pilot study, EBioMedicine 63 (2021), 103154.

[24] J.E. Szulejko, M. McCulloch, J. Jackson, D.L. McKee, J.C. Walker, T. Solouki, Evidence for cancer biomarkers in exhaled breath, Sensor. J. IEEE 10 (2010) 185–210.

[25] H. Amal, D.Y. Shi, R. Ionescu, W. Zhang, Q.L. Hua, Y.Y. Pan, et al., Assessment of ovarian cancer conditions from exhaled breath, Int. J. Cancer 136 (2015) E614–E622.

[26] S. Neethirajan, Recent advances in wearable sensors for animal health management, Sens.Bio Sensing. Res 12 (2017) 15–29.

[27] R. Jansen, J. Wildt, I. Kappers, H. Bouwmeester, J. Hofstee, E. Van Henten, Detection of diseased plants by analysis of volatile organic compound emission, Annu. Rev. Phytopathol. 49 (2011) 157–174.

[28] H. Lin, H. Jiang, S.Y.-S.S. Adade, W. Kang, Z. Xue, M. Zareef, et al., Overview of advanced technologies for volatile organic compounds measurement in food quality and safety, Crit. Rev. Food Sci. Nutr. (2022) 1–23.

[29] A. Garga, M. Akbar, E. Vejerano, S. Narayanan, L. Nazhandali, L.C. Marr, , et al.G. C. Zebra, A mini gas chromatography system for trace-level determination of hazardous air pollutants, Sensor Actuat B-Chem 212 (2015) 145–154.

[30] B.P. Regmi, M. Agah, Micro gas chromatography: an overview of critical components and their integration, Anal. Chem. 90 (2018) 13133–13150.

[31] K.A. Gorder, E.M. Dettenmaier, Portable GC/MS methods to evaluate sources of cVOC contamination in indoor air, Groundwater. Monit. Remediation 31 (2011) 113–119.

[32] Y. Qin, Y.B. Gianchandani, A fully electronic microfabricated gas chromatograph with complementary capacitive detectors for indoor pollutants, Microsystem. Nanoeng. 2 (2016) 1–11.

[33] D. Karakaya, O. Ulucan, M. Turkan, Electronic nose and its applications: a survey, Int. J. Autom. Comput. 17 (2020) 179–209.

[34] Y. Wang, T.S. Raihala, A.P. Jackman, R. St John, Use of Tedlar bags in VOC testing and storage: evidence of significant VOC losses, Environ. Sci. Technol. 30 (1996) 3115–3117.

[35] Y.-H. Kim, K.-H. Kim, S.-H. Jo, E.-C. Jeon, J.R. Sohn, D.B. Parker, Comparison of storage stability of odorous VOCs in polyester aluminum and polyvinyl fluoride Tedlar® bags, Anal. Chim. Acta 712 (2012) 162–167.

[36] E. Woolfenden, Monitoring VOCs in air using sorbent tubes followed by thermal desorption-capillary GC analysis: summary of data and practical guidelines, J. Air Waste Manag. Assoc. 47 (1997) 20–36.

[37] R.W. Bishop, R.J. Valis, A laboratory evaluation of sorbent tubes for use with a thermal desorption gas chromatography-mass selective detection technique, J. Chromatogr. Sci. 28 (1990) 589–593.

[38] S. Zhang, L. Cai, J.A. Koziel, S.J. Hoff, D.R. Schmidt, C.J. Clanton, et al., Field air sampling and simultaneous chemical and sensory analysis of livestock odorants with sorbent tubes and GC–MS/olfactometry, Sensor. Actuator. B Chem. 146 (2010) 427–432.

[39] C.-Y. Peng, S. Batterman, Performance evaluation of a sorbent tube sampling method using short path thermal desorption for volatile organic compounds, J. Environ. Monit. 2 (2000) 313–324.

[40] M. Wilkinson, I.R. White, R. Goodacre, T. Nijsen, S.J. Fowler, Effects of high relative humidity and dry purging on VOCs obtained during breath sampling on common sorbent tubes, J. Breath Res. 14 (2020), 046006.

[41] J.M. Sanchez, R.D. Sacks, On-line multi-bed sorption trap for VOC analysis of large-volume vapor samples: injection plug width, effects of water vapor and sample decomposition, J. Separ. Sci. 28 (2005) 22–30.

[42] H. Lan, K. Hartonen, M.-L. Riekkola, Miniaturised air sampling techniques for analysis of volatile organic compounds in air, TrAC, Trends Anal. Chem. 126 (2020), 115873.

[43] A. Lecharlier, B. Bouyssiere, H. Carrier, I.L. Hécho, Promises of a new versatile field-deployable sorbent tube thermodesorber by application to BTEX analysis in CH4, Talanta Open 4 (2021), 100066.

[44] J. Kwak, M. Fan, C.C. Grigsby, D.K. Ott, Comparison of sampling probe and thermal desorber in hazardous air pollutants on site (HAPSITE) extended range (ER) for analysis of toxic organic (TO)-15 compounds, AIR FORCE RESEARCH LAB WRIGHT-PATTERSON AFB OH HUMAN EFFECTIVENESS DIRECTORATE2014.

[45] A. Stolarczyk, T. Jarosz, Micropreconcentrators: recent progress in designs and applications, Sensors 22 (2022) 1327.

[46] B. Alfeeli, M. Agah, MEMS-based selective preconcentration of trace level breath analytes, IEEE Sensor. J. 9 (2009) 1068–1075.

[47] B. Alfeeli, M. Agah, Toward Handheld Diagnostics of Cancer Biomarkers in Breath: Micro Preconcentration of Trace Levels of Volatiles in Human Breath, 11 ed., Institute of Electrical and Electronics Engineers Inc., 2011, pp. 2756–2762, https://doi.org/10.1109/JSEN.2011.2160390.

[48] B. Alfeeli, M. Agah, Micro preconcentrator with embedded 3D pillars for breath analysis applications, 2008 IEEE Sensors, in: SENSORS 2008, October 26, 2008 - October 29, 2008, Institute of Electrical and Electronics Engineers Inc., Lecce, Italy, 2008, pp. 736–739.

[49] B. Alfeeli, M. Agah, Low pressure drop micro preconcentrators with a cobweb tenax-TA film, 2010 solid-state sensors, actuators, and microsystems workshop, in: June 6, 2010 - June 10, 2010, Transducer Research Foundation, Hilton Head Island, SC, United states, 2010, pp. 166–169.

[50] S. Slimani, E. Bultel, T. Cubizolle, C. Herrier, T. Rousselle, T. Livache, Opto-electronic nose coupled to a silicon micro pre-concentrator device for selective sensing of flavored waters, Chemosensors 8 (2020) 60.

[51] C. Zhan, M. Akbar, R. Hower, N. Nuñovero, J.A. Potkay, E.T. Zellers, A micro passive preconcentrator for micro gas chromatography, Analyst 145 (2020) 7582–7594.

[52] J. Lee, S.-H. Lim, CNT foam-embedded micro gas preconcentrator for low-concentration ethane measurements, Sensors 18 (2018) 1547.

[53] I. Lara-Ibeas, A.R. Cuevas, S. Le Calvé, Recent developments and trends in miniaturized gas preconcentrators for portable gas chromatography systems: a review, Sensor. Actuator. B Chem. 346 (2021), 130449.

[54] B. Alfeeli, D. Cho, M. Ashraf-Khorassani, L.T. Taylor, M. Agah, MEMS-based multi-inlet/outlet preconcentrator coated by inkjet printing of polymer adsorbents, Sensor. Actuator. B Chem. 133 (2008) 24–32.

[55] M. Chowdhury, A. Gholizadeh, M. Agah, Rapid detection of fuel adulteration using microfabricated gas chromatography, Fuel (2021) 286.

[56] B.P. Regmi, R. Chan, A. Atta, M. Agah, Ionic liquid-coated alumina-pretreated micro gas chromatography columns for high-efficient separations, J. Chromatogr. A 1566 (2018) 124–134.

[57] A. Gholizadeh, M. Chowdhury, M. Agah, Ionic liquid stationary phase coating optimization for semi-packed microfabricated columns, J. Chromatogr. A 1647 (2021), 462144.

[58] S.S. Manurkar, Modular GC: A Fully Integrated Micro Gas Chromatography System, Virginia Tech, 2021.

[59] J.J. Whiting, R.D. Sacks, Evaluation of split/splitless operation and rapid heating of a multi-bed sorption trap used for gas chromatography analysis of large-volume air samples, J. Separ. Sci. 29 (2006) 218–227.

[60] D.M. Kialengila, K. Wolfs, J. Bugalama, A. Van Schepdael, E. Adams, Full evaporation headspace gas chromatography for sensitive determination of high boiling point volatile organic compounds in low boiling matrices, J. Chromatogr. A 1315 (2013) 167–175.

[61] M.M. Steeghs, S.M. Cristescu, F.J. Harren, The suitability of Tedlar bags for breath sampling in medical diagnostic research, Physiol. Meas. 28 (2006) 73.

[62] E.M. Gaspar, A.F. Lucena, J.D. da Costa, H.C. das Neves, Organic metabolites in exhaled human breath—a multivariate approach for identification of biomarkers in lung disorders, J. Chromatogr. A 1216 (2009) 2749–2756.

[63] A. Shrivastava, V.B. Gupta, Methods for the determination of limit of detection and limit of quantitation of the analytical methods, Chronicles Young Sci. 2 (2011) 21–25.

[64] M.A.H. Khan, G. ham Nickless, D.E. Shallcross, Sorbent tube sampling and an automated thermal desorption system for halocarbon analysis, TAO: Terr. Atmos. Ocean Sci. 20 (2009) 3.

[65] G. Broadway, A. Tipler, C. Shelton, Ozone precursor analysis using a Thermal Desorption-GC system, PerkinElmer Gas Chromatography White Paper.

[66] B.B. Misra, E. Bassey, M. Olivier, Comparison of a GC-Orbitrap-MS with parallel GC-FID capabilities for metabolomics of human serum, bioRxiv (2019) 740795. https://doi.org/10.1101/740795.

[67] R. Aparicio-Ruiz, D.L. García-González, M.T. Morales, A. Lobo-Prieto, I. Romero, Comparison of two analytical methods validated for the determination of volatile compounds in virgin olive oil: GC-FID vs GC-MS, Talanta 187 (2018) 133–141.